Energy and Buildings 130 (2016) 321–329

Contents lists available at ScienceDirect

Energy and Buildings

journal homepage: www.elsevier.com/locate/enbuild

This research study was conducted using Steril-Aire UVC emitters GTD 40 VO

Effectiveness of an ultraviolet germicidal irradiation system in enhancing cooling coil energy performance in a hot and humid climate

Yi Wang[a,*], Chandra Sekhar[a], William P. Bahnfleth[b], Kok Wai Cheong[a], Joseph Firrantello[b]

[a] Department of Building, School of Design and Environment, National University of Singapore, 4 Architecture Drive, Singapore 117566, Singapore
[b] Indoor Environment Center, Department of Architectural Engineering, The Pennsylvania State University, University Park, PA 16802, USA

ARTICLE INFO

Article history:
Received 26 April 2016
Received in revised form 7 July 2016
Accepted 22 August 2016
Available online 24 August 2016

Keywords:
UVGI
Cooling coil
Coil performance
Energy saving
Hot and humid climate

ABSTRACT

Biological fouling (biofouling) on wetted cooling coil surfaces decreases heat transfer efficiency, increases air-side flow resistance and may eventually lead to more energy consumption by fans and chiller plants. Applying ultraviolet germicidal irradiation (UVGI) systems in air handling units (AHUs) has the potential to clean coils, improve coil performance and save energy. In this study, the effectiveness of a coil irradiation system in improving coil performance and saving energy was investigated through a field test in a hot and humid climate. A commercially available coil irradiation system was installed downstream of a cooling coil in a variable air volume (VAV) AHU. The duration of the field test was 14 months, with four months before UVGI intervention and 10 months after UVGI intervention. The effectiveness of UVGI was evaluated via a "before UV" and "after UV" comparison of coil performance. The coil overall thermal conductance increased by 10% and the pressure drop decreased by 13%, with the improvement being most rapid over the first month after UVGI intervention. Fan energy use fell by 9% over the ten months of UVGI operation. Savings in fan energy were 39% greater than the energy used by the UV lamps.

1. Introduction

1.1. Background

The building sector, the largest energy user in many countries, is also the largest carbon dioxide (CO_2) emitter and the main contributor to climate change [1–3]. Globally, buildings account for around 40% of the total energy consumption and more than 30% of the CO_2 emissions [4]. Heating, Ventilating and Air-Conditioning (HVAC) systems are generally the largest energy end-user in buildings. In Singapore, the building sector accounts for around 31% of the whole country's electricity consumption, of which 60% and 10% of the electricity is used for cooling and ventilation, respectively [5].

The primary purpose of HVAC systems is to provide a comfortable and healthy indoor environment for building occupants by maintaining thermal comfort and indoor air quality (IAQ) at acceptable levels. Cooling coils that transfer heat and mass are key components of HVAC systems. Cooling coils are heat exchangers consisting of rows of finned tubes through which coolant passes and over which warm and humid air passes, as shown in Fig. 1. The compact design of cooling coils makes them susceptible to fouling. Coil fouling such as particulate fouling and biofouling affects cooling coil performance. Properly selected upstream filters can prevent particulate fouling to a large extent. However, it is very challenging to prevent biofouling and this is particularly true in a hot and humid climate like Singapore, where the year-round cool and humid environments around cooling coils make them ideal places for microbes to grow and form colonies.

Fouled coils can become reservoirs of microorganisms [6–11] that distribute biological contaminants into indoor spaces via the ventilation system, resulting in deteriorated IAQ and potentially affecting human health [12–14]. In addition to its negative effects on IAQ and human health, coil fouling may also significantly degrade system performance. Biofouling on coil surfaces decreases the free flow area and increases the pressure drop across coils. Fans consume more energy to overcome the additional pressure to provide indoor spaces with an equivalent amount of air flow for ventilation and thermal control. In addition, the thermal conductivity of biofouling is only around 0.6 W/m K [15,16], more than two orders of magnitude smaller than that of the aluminum coil fin (around 200 W/m K). This huge difference makes biofouling effec-

* Corresponding author.
E-mail address: wangyi13@u.nus.edu (Y. Wang).

http://dx.doi.org/10.1016/j.enbuild.2016.08.063
0378-7788/

Nomenclature

c_p	Specific heat capacity of air [kJ/kg K]
D_i	Tube inside diameter [m]
F	Correction factor for flow arrangement
f_i	Friction factor
h	Heat transfer coefficient [W/m^2 K]
i	Enthalpy [kJ/kg]
k	Thermal conductivity [W/m K]
m	Mass flow rate [kg/s]
ΔP	Pressure drop [Pa]
P_r	Prandtl number
q	Heat transfer rate [kW]
R_e	Reynolds number
T	Temperature [°C]
UA	Overall enthalpy-based thermal conductance for cooling and dehumidifying coils [kg/s]
u	Velocity [m/s]
W	Fan power [kW]
x	Correction factor for temperature
AFTMS	Air flow temperature measuring station
AHU	Air handling unit
BMS	Building management system
CCSIM	Simple cooling coil
CO_2	Carbon dioxide
DNA	Deoxyribonucleic acid
HVAC	Heating, ventilating and air-conditioning
IAQ	Indoor air quality
ID-UVGI	In-duct UVGI
IEP	Inverse EnergyPlus
LMED	Log mean enthalpy difference
LMTD	Log mean temperature difference
RNA	Ribonucleic acid
UR-UVGI	Upper-room UVGI
UVC	Ultraviolet C
UVGI	Ultraviolet germicidal irradiation
VAV	Variable air volume

Subscripts

a	Air
d_p	Dew-point
sat	Saturation
w	Water
in	Coil inlet
out	Coil outlet
mean	Mean value
0	Operating condition
1	Reference condition

Greek symbols

η_f	Fin efficiency
ρ	Density [kg/m^3]
μ	Dynamic viscosity [Pa s]

tive thermal insulation, impeding the heat transfer from warm air to coolant and decreasing the air-side heat transfer coefficient. In order to overcome the additional thermal insulation and maintain the same supply air set point temperature in fouling conditions, chilled water systems usually react in two different ways which are associated with more energy usage. The first way is to increase the chilled water flow rate without changing the chilled water supply conditions, causing chilled water pumps to run harder and consume more energy. This occurs automatically. The second way is to lower the chilled water supply temperature, causing chillers to run in non-optimum conditions with reduced coefficient of performance. Reset of chilled water temperature set point is normally done by operator intervention.

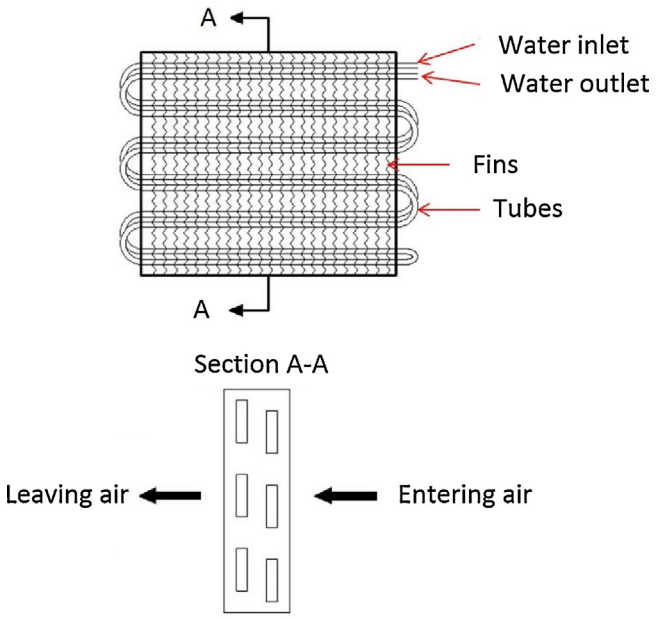

Fig. 1. A schematic of a 2-row cooling coil.

Annual or semi-annual coil cleaning is commonly recommended by manufacturers to prevent coils from fouling heavily and to ensure that they operate under optimum conditions. The most widely used coil cleaning methods are chemical cleaning and high-pressure water cleaning, frequently in conjunction. For chemical cleaning, chemicals need to be removed thoroughly to avoid potential danger to both indoor occupants and service personnel. For high pressure water cleaning, it is very possible for fouling to be driven into coils, making it out of sight and even harder to be removed. Regardless of which method of conventional coil cleaning is used, facility shutdown is required and cost is significant.

Ultraviolet germicidal irradiation (UVGI) is a well-known technology with over a century of history that uses Ultraviolet C (UVC) radiation at the wavelength of 253.7 nm to inactive microorganisms by altering the molecular bonds and structure of their Deoxyribonucleic acid (DNA) and Ribonucleic acid (RNA). The altered DNA and RNA prevent microorganisms from reproducing. Different types of UVGI systems have been widely used in real world applications, including but not limited to upper-room UVGI (UR-UVGI), in-duct UVGI (ID-UVGI) and UVGI coil irradiation systems. For UR-UVGI, UV radiation is confined in the upper space of rooms above the occupied zone to provide air disinfection when the air passes through the irradiated zone. For ID-UVGI, UV lamps are installed in AHUs for the purpose of air treatment. For coil irradiation systems, UV lamps are installed in AHUs to provide surface disinfection for coil surfaces. In recent years, there is a growing interest in government agencies and HVAC communities for coil irradiation systems due to their potential to improve coil performance, maintain coil condition, save energy and improve IAQ.

1.2. Literature review on coil fouling

Multiple studies on the effects of particulate fouling are available in the scientific literature. Bell and Groll [17], in a laboratory test, found a more than 200% increase in the air-side pressure drop and a more than 10% decrease in the heat transfer rate with the injection of ASHRAE Standard Dust and Arizona Road Test Dust, respectively. Yang et al. [18] injected 600 g of dust upstream of coil-filter combi-

nations in a laboratory test to investigate the effects of particulate fouling. Increase in the pressure drop, ranging from 6% to 200%, was observed in different coil-filter combinations. Impacts on the air-side heat transfer coefficient were different for different coil-filter combinations, ranging from −14% to 4%. They found enhancement in the air-side heat transfer coefficient for a certain coil with good filtration and speculated that, in some cases, the presence of dust created additional turbulence which could enhance heat transfer. It was also found that the majority of dust fouling was on the leading edges of coils. Ahn et al. [19] collected field-installed evaporators and tested their performance in a laboratory environment. 10–15% reduction in cooling capacity of heat exchangers with 7 years of usage was found.

Biofouling differs from particulate fouling in many aspects, including fouling site, fouling material and fouling formation conditions. As reported by Yang et al. [18], the majority of particulate fouling was found on the leading edges of coils. Luongo and Miller [20] found that microbial growth on coil surfaces was dependent on coil operating conditions, with higher microbial loading on downstream coil surfaces in condensing conditions and, conversely, higher loading on upstream surfaces in dry conditions.

Peer-reviewed studies on the effects of biofouling on cooling coil performance are quite limited in the scientific literature. Pu et al. [21] showed 21.8–41.3% increase in the pressure drop at face velocities ranging from 0.5 m/s to 2.0 m/s, and 7.2–15.9% reduction in the air-side heat transfer coefficient at the face velocity of 2.0 m/s through a laboratory test by artificially growing microorganisms on coil surfaces.

1.3. Motivation and objectives

Although a large body of anecdotal evidence from real-world coil irradiation systems show promising energy saving potential, very few relevant peer-reviewed studies can be found in the scientific literature [22]. In order to form a better understanding of coil irradiation system characteristics, it is important to investigate their effectiveness in improving coil performance and energy saving potential in real-world applications on the basis of a sufficiently long period of UVGI intervention. In this study, the effectiveness of a coil irradiation system is investigated in a laboratory building in Singapore. Singapore is near the equator and has a typically tropical climate, with high temperatures and humidity levels. According to Meteorological Service Singapore [23], temperatures and relative humidities vary very little from month to month from 1982 to 2014. The average monthly temperatures range from 26.0 °C to 27.8 °C and the mean annual relative humidity is 84.1%. The year-round cooling and humidity load promote microbial growth on the coil. The whole duration of UVGI intervention is 10 months. The primary focus of this study is the comparison of “before UV” and “after UV” coil performance indicators such as overall enthalpy-based thermal conductance (UA value), air-side pressure drop and fan power, which is a crucial step towards the evaluation of energy saving potential of coil irradiation systems.

2. Methodology

This study is a field investigation aiming to characterize the effectiveness of coil irradiation systems under actual working conditions. The methodology consists of five parts: (1) cooling coil selection and UVGI system; (2) energy related measurements for the cooling coil; (3) “before UV” and “after UV” comparison of coil performance; (4) pre-processing of data; and (5) uncertainty analysis.

Table 1
Summary of the coil geometry.

Parameter	Value
Number of rows	8
Number of circuits	76
Number of tubes per row	38
Number of tubes per circuit	4
Fin thickness [mm]	0.115
Spacing between fins [mm]	2.425
Fins per inch	10
Fin height [mm]	1206.0
Tube length [mm]	1517.0
Outside tube diameter [mm]	12.70
Inside tube diameter [mm]	12.02
Tube thickness [mm]	0.34
Longitudinal tube pitch [mm]	27.50
Transverse tube pitch [mm]	31.75

2.1. Cooling coil selection and UVGI system

It is important to ensure that the cooling coil under investigation is sufficiently fouled so that the effectiveness of coil irradiation systems can be tested clearly. There is no well-defined quantitative standard for defining a fouled coil. Cooling coil was selected by the investigators based on two selection criteria: visual evidence of fouling and history of complaints from occupants served by the coil. Generally, fouled cooling coils have visible fouling material on coil surfaces, which can be easily observed. In addition, odor complaints from occupants can be an indication of coil fouling. Based on the above two criteria, a cooling coil in continuous operation in a VAV AHU in a laboratory building was selected for this study. The selected coil was not heavily fouled. It was maintained according to a regular cleaning schedule. The last maintenance of the coil took place 6 months prior to the beginning of the study. The reason for choosing a regularly maintained coil is to have a fouling condition representative of typical performance, rather than exaggerating the impacts of coil irradiation systems based on the impacts on coils with heavy fouling. A summary of coil information for the selected system is listed in Table 1.

In this study, a commercially available coil irradiation system was installed downstream of the cooling coil and above the drain pan. Two low pressure mercury vapor double-ended germicidal UV lamps (GTD 40 VO) were installed inside the AHU as shown in Figs. 2 and 3. The input power of each lamp is 109 W. For coil irradiation systems, UV lamps can be installed either on the upstream or downstream side or on both sides of cooling coils. Positioning UV lamps on both sides may be the best approach for coil surface disinfection as radiation from one side only may be greatly attenuated before reaching the opposite surface of the coil. In most cases, UV lamps are installed on the downstream side because the condensate water moves towards the downstream side and the condensate drain pan can be irradiated at the same time.

2.2. Energy related measurements for the cooling coil

Air-side and water-side parameters of the cooling coil such as air flow rate, on/off coil temperatures, on/off coil relative humidities, pressure drop, chilled water flow rate, fan power, and chilled water supply/return temperatures were continuously measured by relevant sensors and recorded by a building management system (BMS). Data were logged as 6 min average data. During the period of measurements in this study, on-coil temperatures ranged from 21.5 °C to 28.0 °C; on-coil relative humidities ranged from 45% to 81%.

The airflow was measured by an electronic thermal dispersion type airflow temperature measuring station (AFTMS, EAMP) with a grid of 2 × 2 (2 probes with 2 sensors per probe). The mean airflow

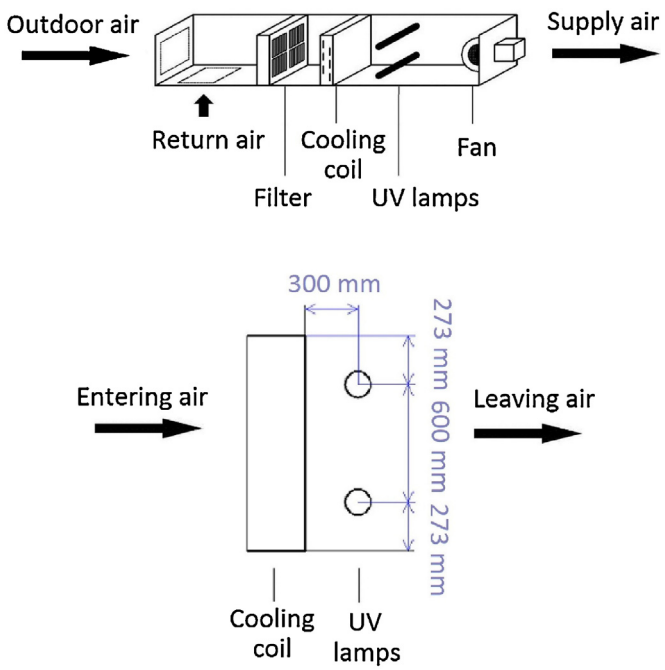

Fig. 2. A schematic of the coil irradiation system.

over the grid was used for further calculation of air-side heat transfer rate. The air temperatures upstream and downstream of the cooling coil were measured by rigid averaging sensor probes fully covered by continuous sensing element (ST-AV81H). The mean air temperature was used in the calculation of enthalpy. Water temperature was measured by an immersion sensor (ST-W71E-XW).

Table 2
Summary of the uncertainties of measured values.

Parameter	Uncertainty
Air flow rate [m/s]	±2% of reading
Air temperature [°C]	±0.15
Water temperature [°C]	±0.2
Relative humidity [%]	0–90: ±1.5; 90–100: ±2.5
Pressure drop [Pa]	±0.4% of reading
Water flow rate [L/s]	±0.25% of reading
Fan power (kW)	±0.1% of reading

The relative humidity was also measured upstream and downstream of the cooling coil using humidity transmitters (HMT 120). The pressure drop across the cooling coil was measured by using a differential pressure transmitter (CXLdp). The chilled water flow rate was measured with an electromagnetic flow sensor (SITRANS F M MAG 5100 W). Table 2 summarizes the uncertainties of the measured values.

2.3. "Before UV" and "after UV" coil performance comparison

In order to characterize the effectiveness of coil irradiation systems in improving energy performance of cooling coils, a "before UV" and "after UV" comparative approach was used. Field measurements commenced around four months before turning on the UV lamps and continued for 10 months subsequently. The measurement schedule is summarized in Table 3. During the UV irradiation period, no other intervention took place in the coil. Upstream filters were replaced according to the normal maintenance schedule. Hence, any variation in coil performance after UV intervention can only be attributed to the effects of the coil irradiation system.

Three key indicators of coil performance: overall enthalpy-based thermal conductance (UA value), air-side pressure drop and

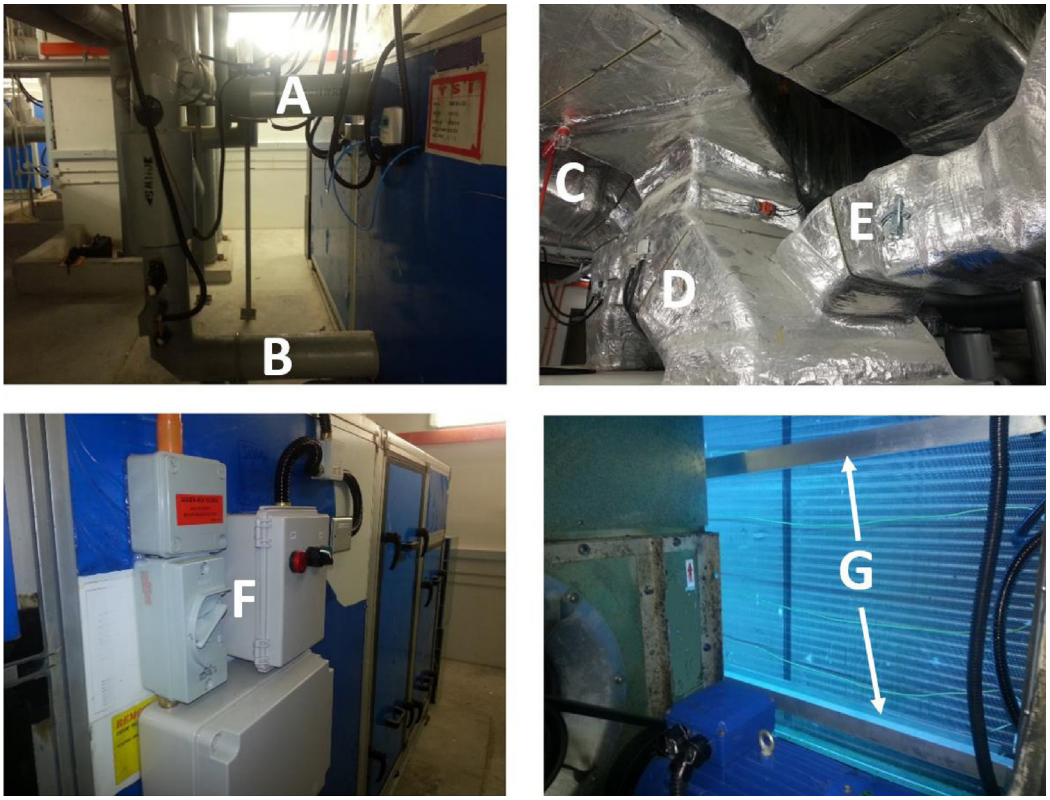

Fig. 3. Test apparatus (A: Chilled water return pipe; B: Chilled water supply pipe; C: Supply air duct; D: Return air duct; E: Outdoor air duct; F: UV switch and interlock; G: UV lamps).

Table 3
Summary of the measurement schedule.

UV status	Time
Before UV	2013/11/01–2014/02/25
Turning on UV	2014/02/26
After UV	2014/02/26–2014/12/31

fan power were examined. For pressure drop and fan power, a classic power law relationship was employed to correlate them with face velocity, as shown in Eqs. (1) and (2), respectively. The regression results make it possible to quantify the effectiveness of coil irradiation systems in reducing pressure drop and fan power at different face velocities.

$$\Delta P = b u_a^c \tag{1}$$

$$W = d u_a^e \tag{2}$$

where u_a is the face velocity, ΔP is the air-side pressure drop, W is the fan power, b,c,d,e are the coefficients.

The UA value is a function of coil operating conditions. Different operating conditions will result in different UA values, making direct "before UV" and "after UV" comparison in a field test challenging. In order to evaluate the change in UA, it is necessary to compare UA values at a reference operating condition before and after application of UVGI. According to the existing literature, there is no published method capable of converting UA values from operating conditions to a reference condition. However, there are a couple of methods (EnergyPlus method [24] and Morisot method [25]) to calculate UA values at different operating conditions given a UA value at a reference condition. They are mainly developed for energy simulation tools to simulate yearly energy consumption. EnergyPlus method utilizes Simple Cooling Coil (CCSIM) model to calculate the overall UA value at a reference condition and then converts the UA value from a reference condition to different operating conditions according to different water-side and air-side coil inlet conditions. The CCSIM model, presented in ASHRAE HVAC2 Toolkit, was developed by Brandemuehl et al. [26] to simulate coils when detailed geometrical data is not available. In this study, the method used in EnergyPlus is inversely employed for calculating the UA value at a reference condition. Given the UA values at varying operating conditions, the UA value at the reference condition is calculated via an inverse application of the EnergyPlus model. This approach was previously applied with good results to analysis of data from a coil irradiation installation in Tampa, FL in the United States by Firrantello et al. [27].

There are two reasons for choosing the inverse EnergyPlus (IEP) method over Morisot method. The first reason is that the IEP method considers four parameters (water/air flow rate, chilled water supply temperature and entering air temperature) during conversion, while Morisot method only considers two (water/air flow rate). The second reason is to keep conversion method consistent when it comes to conducting simulation in EnergyPlus at a later stage. The procedure of IEP method is listed below. Subscript 0 and 1 mean operating conditions and the reference condition, respectively.

1. Calculate the overall enthalpy-based UA ($(UA)_0$) at operating conditions
2. Calculate the temperature-based air-side UA ($(\eta_f(hA)_a)_0$) and water-side UA ($(hA)_{w,0}$) at operating conditions
3. Calculate the air-side correction factor x_a and water-side correction factor x_w
4. Calculate the temperature-based air-side UA ($(\eta_f(hA)_a)_1$) and water-side UA ($(hA)_{w,1}$) at the reference condition
5. Calculate the overall enthalpy-based UA ($(UA)_1$) at the reference condition

The enthalpy-based UA values at operating conditions can be determined from measured data using the log mean enthalpy difference method, described in Eqs. (3) and (4). Using log mean enthalpy difference (LMED) method in this study is due to that the cooling coil under investigation is associated with both sensible and latent cooling. For heat exchangers with only sensible load, the log mean temperature difference (LMTD) method will be used.

$$(UA)_0 = \frac{q}{F \cdot LMED} \tag{3}$$

$$LMED = \frac{(i_{a,in,0} - i_{w,out,0}) - (i_{a,out,0} - i_{w,in,0})}{\ln \frac{i_{a,in,0} - i_{w,out,0}}{i_{a,out,0} - i_{w,in,0}}} \tag{4}$$

where q is the heat transfer rate of the cooling coil, $LMED$ is the log mean enthalpy difference, $i_{a,in,0}$ and $i_{a,out,0}$ are, respectively, the entering and leaving air enthalpy, $i_{w,in,0}$ and $i_{w,out,0}$ are, respectively, the saturated air enthalpy at chilled water supply and return temperature, and F is the correction factor for flow arrangement. Coils with two or more rows can be considered as counter flow heat exchangers for which the correction factor F is unity [28]. It is to be noted that F is dimensionless, heat transfer rate q has a unit of kW and $LMED$ has a unit of kJ/kg. Hence, the unit of overall enthalpy-based thermal conductance UA is kW/(kJ/kg), representing the rate of heat transfer per unit log mean enthalpy difference. After unit conversion, kW/(kJ/kg) is reduced to kg/s. kg/s is used as the unit of overall enthalpy-based UA in this paper for simplification purpose.

The enthalpy-based UA is related to the conventional temperature-based UA by the specific heat. Hence, the enthalpy-based thermal resistance balance for a cooling coil at operating conditions is described in Eq. (5), whose derivation procedure can be found in HVAC2 Toolkit [26].

$$\frac{1}{(UA)_0} = \frac{c_{p,sat,0}}{(hA)_{w,0}} + \frac{c_{p,a}}{(\eta_f(hA)_a)_0} \tag{5}$$

where $\frac{1}{(UA)_0}$ is the overall enthalpy-based thermal resistance between air and water, $\frac{c_{p,sat,0}}{(hA)_{w,0}}$ and $\frac{c_{p,a}}{(\eta_f(hA)_a)_0}$ are the water-side and air-side thermal resistances, respectively; $c_{p,a}$ is the specific heat of dry air and $c_{p,sat,0}$ is an effective specific heat capacity of saturated air, defined by Eq. (6).

$$c_{p,sat,0} = \frac{i_{a,in,dp,0} - i_{w,in,0}}{T_{a,in,dp,0} - T_{w,in,0}} \tag{6}$$

where $i_{a,in,dp,0}$ is the saturated air enthalpy at the dew-point temperature of entering air ($T_{a,in,dp,0}$) and $T_{w,in,0}$ is the chilled water supply temperature. Compared with the air-side and water-side convective resistances, the tube conductive resistance is much lower. Hence, it can be neglected in the thermal resistance balance expressed above by Eq. (5).

The water-side heat transfer coefficient is calculated using the Gnielinski correlation [29], which is valid for smooth tubes over a large Reynolds number range including the transition region. It is valid for $0.5 \le \mathrm{P_r} \le 2000$ and $3000 \le \mathrm{R_e} \le 5 \times 10^6$.

$$h_{w,0} = \left(\frac{k_w}{D_i}\right) \frac{(Re_{D_i} - 1000) Pr (f_i/2)}{1 + 12.7\sqrt{f_i/2}(Pr^{2/3} - 1)} \tag{7}$$

where D_i is the inside tube diameter, Pr is the Prandtl number, k_w is the thermal conductivity of water, Re is the Reynolds number defined in Eq. (8), and f_i is the friction factor defined in Eq. (9).

$$Re_{D_i} = \rho_w u_w D_i / \mu_w \tag{8}$$

$$f_i = (1.58 \ln(Re_{D_i}) - 3.28)^{-2} \tag{9}$$

where ρ_w is the density of water, u_w is the water velocity and μ_w is the dynamic viscosity of water.

Table 4
The reference condition of the cooling coil.

Parameter	$T_{a,in,1}$ [°C]	$RH_{in,1}$ [%]	$u_{a,1}$ [m/s]	$T_{w,in,1}$ [°C]	$Q_{w,1}$ [L/s]
Value	26.7	50.8	2.12	7.0	5.118

The water-side heat transfer area can be calculated from tube geometrical data. Hence, the air-side UA $(\eta_f(hA)_a)_0$ can be calculated from Eq. (5).

The air-side and water-side correction factor can be calculated from entering air temperature and chilled water supply temperature, respectively. They account for the effects of temperature on air and water thermal properties.

$$x_a = 1 + 4.769 \cdot 10^{-3}(T_{a,in,1} - T_{a,in,0}) \tag{10}$$

$$x_w = 1 + \left(\frac{0.014}{1 + 0.014T_{w,in,0}}\right)(T_{w,in,1} - T_{w,in,0}) \tag{11}$$

where x_a is the air-side correction factor, x_w is the water-side correction factor, $T_{a,in}$ is the entering air temperature, and $T_{w,in}$ is the chilled water supply temperature.

The air-side UA $(\eta_f(hA)_a)_1$ and water-side UA $(hA)_{w,1}$ at the reference condition can be derived from Eqs. (12) and (13).

$$(\eta_f(hA)_a)_1 = x_a\left(\frac{m_{a,1}}{m_{a,0}}\right)^{0.8}(\eta_f(hA)_a)_0 \tag{12}$$

$$(hA)_{w,1} = x_w\left(\frac{m_{w,1}}{m_{w,0}}\right)^{0.85}(hA)_{w,0} \tag{13}$$

where m_a is the air mass flow rate and m_w is the water mass flow rate.

Hence, the overall enthalpy-based UA value at the reference condition can be calculated from Eqs. (14) and (15)

$$\frac{1}{(UA)_1} = \frac{c_{p,sat,1}}{(hA)_{w,1}} + \frac{c_{p,a}}{(\eta_f(hA)_a)_1} \tag{14}$$

$$c_{p,sat,1} = \frac{i_{a,in,dp,1} - i_{w,in,1}}{T_{a,in,dp,1} - T_{w,in,1}} \tag{15}$$

The reference condition of the cooling coil is listed in Table 4.

2.4. Pre-processing of data

In the field test, the coil was in continuous operation and data was collected continuously. The advantage of a field test is the ability to capture the nature of the real-world condition, while the disadvantage is the associated significant data noise, which needs to be evaluated and processed properly before analysis. There are two steps during data pre-processing. The first step is to remove zero or negative values, which may be collected during AHU shutdown or result from sensor signal transmission problems. The second step is to remove additional unrealistic data, such as leaving air temperature higher than entering air temperature, or chilled water return temperature lower than chilled water supply temperature.

2.5. Uncertainty analysis

The uncertainty of a calculated variable is determined by combining the uncertainties in the independently measured variables through uncertainty propagation [30], as shown in Eq. (16).

$$U_R = \left[\sum_{i=1}^{n}\left(\frac{\partial R}{\partial X_i}\cdot U_{X_i}\right)^2\right]^{1/2} \tag{16}$$

Table 5
UA at the reference condition (mean ± uncertainty).

	Before UV	After UV	Increase
UA [kg/s]	7.632 ± 0.007	8.361 ± 0.005	9.552% ± 0.120%

where U_{X_i} is the uncertainty in a measured variable X_i, R is the function of the measured variables, and U_R is the uncertainty in the calculated variable.

Once the uncertainty of every UA is determined, the uncertainty of the mean of UA can be determined using the same uncertainty propagation method, as described in Eqs. (17)–(20).

$$UA_{mean} = \frac{\sum_{i=1}^{n} UA_i}{n} = \frac{UA_1 + UA_2 + \cdots + UA_n}{n} \tag{17}$$

$$U_{UA_{mean}} = \sqrt{\left(\frac{\partial UA_{mean}}{\partial UA_1}\right)^2 U_{UA_1}^2 + \left(\frac{\partial UA_{mean}}{\partial UA_2}\right)^2 U_{UA_2}^2 + \cdots \left(\frac{\partial UA_{mean}}{\partial UA_n}\right)^2 U_{UA_n}^2} \tag{18}$$

$$\frac{\partial UA_{mean}}{\partial UA_1} = \frac{\partial UA_{mean}}{\partial UA_2} = \cdots = \frac{\partial UA_{mean}}{\partial UA_n} = \frac{1}{n} \tag{19}$$

$$U_{UA_{mean}} = \frac{1}{n}\sqrt{\sum_{i=1}^{n} U_{UA_i}^2} \tag{20}$$

3. Results

3.1. Overall enthalpy-based thermal conductance (UA)

The "before UV" and "after UV" comparison of UA values at the reference condition is shown in Fig. 4. As can be seen in Fig. 4, there is a sharp break at around 5 kg/s at the lower end, and another sharp break at around 12 kg/s at the higher end for both "before UV" and "after UV" distribution. The extreme values at the upper end are associated with higher-than-normal chilled water flow rate, which may be collected during periods of significant water-side flow rate fluctuation. The extreme values at the lower end are associated with very high chilled water supply temperature, which may be collected when a chiller was off or a pump was just turned on. These extreme values were collected during extreme or unsteady operating conditions and should be removed to refine the data set so that it can better represent normal operating conditions. The outlier elimination removed around 700 data points, approximately 0.7% of the total after pre-processing. The difference between "before UV" and "after UV" mean UA value after outlier removal is given in Table 5. UA value increases by approximately 10% at the reference condition after applying the coil irradiation system.

The small uncertainty of the mean UA is due to the fact that the mean of multiple measurements of a given quantity will converge to the expected value regardless of the uncertainty of the individual measurement due to the law of large numbers. The reported UA is mean value averaged over around 94,000 data points.

3.2. Pressure drop

In Fig. 5, a distinct reduction in pressure drop occurs after UV intervention. This is attributed to an increase in the free flow area of the cooling coil with the biofouling being reduced due to the germicidal effects of UVGI, and consequently, the pressure drop being reduced. The regression results are reasonable for a field test with R^2 being 0.88 and 0.95 for "before UV" and "after UV" regression, respectively. At the reference face velocity of 2.12 m/s, the pressure drop decreases by about 13%, from 40.6 Pa to 35.3 Pa.

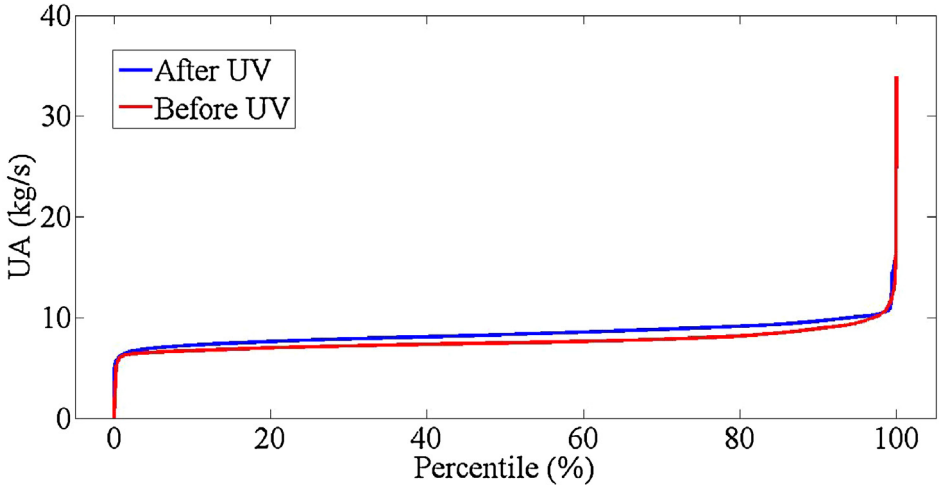

Fig. 4. Comparison of UA at the reference condition.

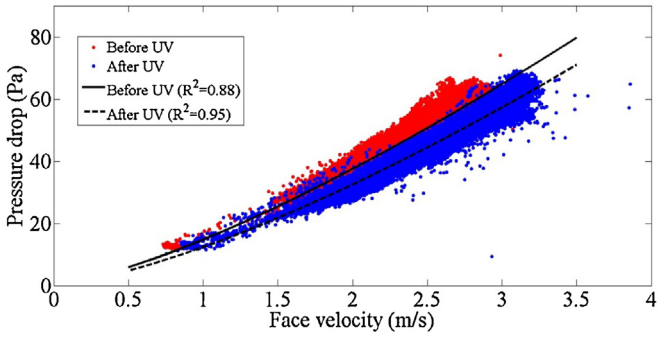

Fig. 5. Pressure drop vs. face velocity.

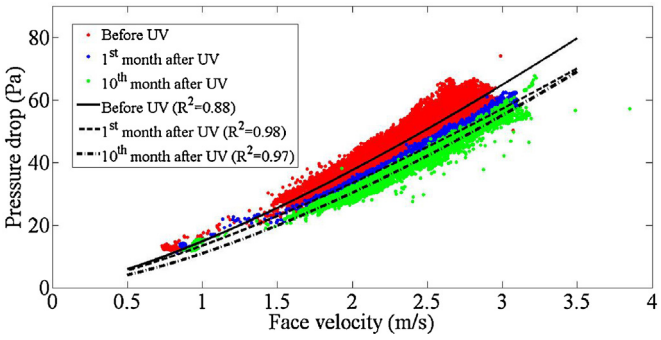

Fig. 6. Pressure drop vs. face velocity (breakdown).

Although a clear and distinct reduction in pressure drop can be observed after UV intervention, the "after UV" regression line represents the average condition over ten months. In order to differentiate the effects of the coil irradiation system at different stages, the "after UV" data is divided into ten different one-month groups. The 1st group (1st month after UV) and 10th group (10th month after UV) are compared with "before UV" data, as shown in Fig. 6.

As can be seen in Fig. 6, the regression results are quite good with R^2 being 0.98 and 0.97 for "1st month after UV" and "10th month after UV" scenario, respectively. At the reference face velocity of 2.12 m/s, the average pressure drop after UV is 36.1 Pa over the 1st month and 33.0 Pa over the 10th month. Compared to the "before UV" condition, the percentage reductions are 11% and 19%, respectively.

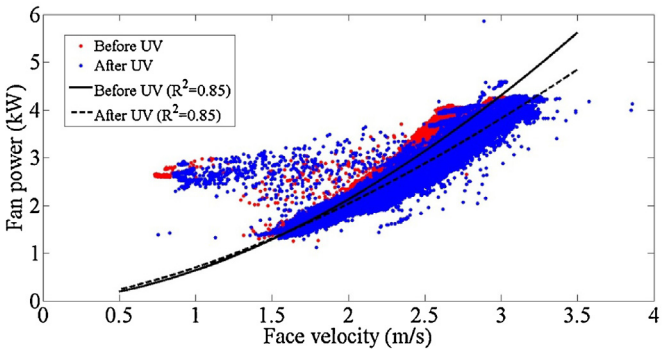

Fig. 7. Fan power vs. face velocity.

Table 6 summarizes the pressure drop at the reference face velocity under different scenarios. As presented in Table 6, the percentage reduction in pressure drop over a period of ten months after UV is 13%. However, the reduction is already as high as 11% over the first month, indicating that the coil irradiation system is able to reduce the pressure drop for this fouled coil rapidly. Although a 19% reduction can be achieved after ten months of UV intervention, it takes nine months to achieve this additional 8% reduction.

3.3. Fan power

In VAV AHUs, when fouling materials accumulate on cooling coil surfaces, fans have to work harder to overcome the increased pressure so as to provide the same amount of airflow, which can result in more energy use by the fans. In Fig. 7, a distinct reduction in fan power can be observed after UV, which is in good agreement with the aforementioned reduction in pressure drop. It reduces by approximately 5%, from 2.35 kW to 2.23 kW, at the reference face velocity of 2.12 m/s. In order to estimate the fan energy savings for the whole period of ten months after UV, the "before UV" condition is assumed to be the baseline. It is to be noted that this is a conservative assumption because fan power is likely to continuously increase over the next ten months in normal operating environment without UV as the coil fouls. For every 6-min average data point, it is assumed that face velocity is constant, and the fan energy savings are evaluated based on the "before UV" and "after UV" regression results. The fan energy savings of every 6 min are summed over ten months, and the result is the estimated fan energy savings over a period of ten months after UV intervention. Following the above assumption, the fan energy use reduces by

Table 6
Pressure drop at the face velocity of 2.12 m/s under different scenarios.

	Before UV	After UV	1st month after UV	10th month after UV
Pressure drop at 2.12 m/s [Pa]	40.6	35.3	36.1	33.0
Reduction	–	13%	11%	19%

Table 7
A summary of regression coefficients.

	Coefficients			
	b	*c*	*d*	*e*
Before UV	14.78	1.345	0.6388	1.736
After UV	12.36	1.396	0.6977	1.547
1st month after UV	13.38	1.322	–	–
10th month after UV	10.92	1.472	–	–

approximately 9%, from 22587 kWh to 20532 kWh. The calculated fan energy savings are 2055 kWh. UV lamps consume energy as well. The input power of UV lamps used in this study is 109 W per lamp. Over the period of ten months, the energy use by two lamps is 1476 kWh. Thus, the savings in fan energy alone are 39% greater than the energy used by the UV lamps.

The regression coefficients in Eqs. (1) and (2) are summarized in Table 7.

4. Discussion

The results presented in this paper demonstrate the effectiveness of UVGI systems in enhancing coil performance in buildings and its associated energy saving potential in a hot and humid climate. In order to capture the nature of real fouling conditions and eliminate the bias resulting from investigating heavily fouled cooling coils, a cooling coil operating in a laboratory building and maintained on a regular schedule is tested in this study. For a field test, the inability to control test conditions poses a great challenge to make a valid "before UV" and "after UV" comparison of UA value. The Inverse EnergyPlus method used to convert UA values under different operating conditions to a value at a single reference condition is a promising method for comparing coil heat transfer performance before and after UV intervention. Proper data preprocessing to eliminate irrelevant and unrealistic data is required. The 10% increase in UA value after UV intervention reveals the potential of the coil irradiation system to improve coil heat transfer performance, which may eventually lead to energy savings on chiller side.

For this specific coil, the reduction in pressure drop and fan power after UV intervention is very distinct, indicating the coil irradiation system's potential to reduce flow resistance and save fan energy. At the reference face velocity of 2.12 m/s, the average pressure drop reduction over a period of ten months is 13% and an 11% reduction is achieved after only one month of UV intervention, suggesting that the coil irradiation system is able to rapidly reduce pressure drop. Although the additional reduction is only 8% over the next nine months, the pressure drop is kept at a lower level constantly, indicating the ability of the coil irradiation system to maintain coil performance for several months and its potential to decrease coil maintenance frequency. In addition, savings in fan energy alone for this coil exceed the energy used by UV lamps, showing that the application of coil irradiation systems can be an energy-efficient way to improve and maintain coil performance and reduce energy cost.

The results of this study are based on a coil with regular cleaning. The major finding of this study is the evidence of energy saving potential by using coil irradiation systems even for such coils. Improvement could be significantly greater for a coil that is otherwise poorly maintained. However, the results reported in this paper are only limited to a hot and humid climate, a specific coil geometry and a specific coil irradiation system. In a hot and humid climate, the coil is likely to be wet whenever operating, which promotes biofouling. Less biofouling would be expected on coils in temperate climates. Coil geometric dimensions such as coil depth and fin density vary and may be significant. To date, the design irradiance for coil irradiation systems is set by empirical guidelines. No studies quantifying the effects of irradiance on performance, although it is easy to envision that there is a threshold value below which a system would be ineffective. Future studies are necessary to establish a relationship between the effectiveness of coil irradiation systems and the above factors.

5. Conclusions

The main conclusions of this field study on the effectiveness of a coil irradiation system in improving coil performance and saving energy in a hot and humid climate are:

- The application of a coil irradiation system for a period of ten months increases coil overall enthalpy-based thermal conductance by 10% and reduces pressure drop by 13%.
- Improvement in coil performance is most rapid initially and may continue for several months.
- Fan energy use reduces by 9% over a period of ten months with UV irradiation. Savings in fan energy are 39% greater than the energy used by the UV lamps; there can be a net reduction in energy cost after applying a coil irradiation system.
- The Inverse EnergyPlus method is a promising method to investigate coil heat transfer performance at a reference condition when there is lack of control over coil inlet conditions.

Acknowledgements

The present study is part of a collaborative research project between National University of Singapore and Pennsylvania State University. The financial support of the National University of Singapore in the form of research grant RP 296-000-132-112 is gratefully acknowledged. Suggestions from Professor William P. Bahnfleth's team from Pennsylvania State University on instrumentation, experimental design and experimental protocol are greatly appreciated.

References

[1] J. Xia, T. Hong, Q. Shen, W. Feng, L. Yang, P. Im, A. Lu, M. Bhandari, Comparison of building energy use data between the United States and China, Energy Build. 78 (2014) 165–175.
[2] L. Yang, H. Yan, J.C. Lam, Thermal comfort and building energy consumption implications—a review, Appl. Energy 115 (2014) 164–173.
[3] L. Pérez-Lombard, J. Ortiz, C. Pout, A review on buildings energy consumption information, Energy Build. 40 (3) (2008) 394–398.
[4] A. Costa, M.M. Keane, J.I. Torrens, E. Corry, Building operation and energy performance: monitoring, analysis and optimisation toolkit, Appl. Energy 101 (2013) 310–316.
[5] K.J. Chua, S.K. Chou, W.M. Yang, J. Yan, Achieving better energy-efficient air conditioning—a review of technologies and strategies, Appl. Energy 104 (2013) 87–104.
[6] P. Hugenholtz, J.A. Fuerst, Heterotrophic bacteria in an air-handling system, Appl. Environ. Microbiol. 58 (12) (1992) 3914–3920.

[7] E. Levetin, R. Shaughnessy, C.A. Rogers, R. Scheir, Effectiveness of germicidal UV radiation for reducing fungal contamination within air-handling units, Appl. Environ. Microbiol. 67 (8) (2001) 3712–3715.
[8] D. Menzies, J. Popa, J.A. Hanley, T. Rand, D.K. Milton, Effect of ultraviolet germicidal lights installed in office ventilation systems on workers' health and wellbeing: double-blind multiple crossover trial, Lancet 362 (9398) (2003) 1785–1791.
[9] M.Y. Menetrez, K.K. Foarde, T.R. Dean, D.A. Betancourt, The effectiveness of UV irradiation on vegetative bacteria and fungi surface contamination, Chem. Eng. J. 157 (2–3) (2010) 443–450.
[10] D. Menzies, J. Pasztor, T. Rand, J. Bourbeau, Germicidal ultraviolet irradiation in air conditioning systems: effect on office worker health and wellbeing: a pilot study, Occup. Environ. Med. 56 (6) (1999) 397–402.
[11] R.M. Ryan, G.E. Wilding, R.J. Wynn, R.C. Welliver, B.A. Holm, C.L. Leach, Effect of enhanced ultraviolet germicidal irradiation in the heating ventilation and air conditioning system on ventilator-associated pneumonia in a neonatal intensive care unit, J. Perinatol. 31 (9) (2011) 607–614.
[12] M.J. Mendell, M. Cozen, Q. Lei-Gomez, H.S. Brightman, C.A. Erdmann, J.R. Girman, S.E. Womble, Indicators of moisture and ventilation system contamination in U.S. office buildings as risk factors for respiratory and mucous membrane symptoms: analyses of the EPA BASE data, J. Occup. Environ. Hyg. 3 (5) (2006) 225–233.
[13] M.J. Mendell, Q. Lei-Gomez, A.G. Mirer, O. Seppanen, G. Brunner, Risk factors in heating, ventilating, and air-conditioning systems for occupant symptoms in US office buildings: the US EPA BASE study, Indoor Air 18 (4) (2008) 301–316.
[14] M.J. Mendell, G.M. Naco, T.G. Wilcox, W.K. Sieber, Environmental risk factors and work-related lower respiratory symptoms in 80 office buildings: an exploratory analysis of NIOSH data, Am. J. Ind. Med. 43 (6) (2003) 630–641.
[15] L.F. Melo, M.J. Vieira, Physical stability and biological activity of biofilms under turbulent flow and low substrate concentration, Bioprocess. Eng. 20 (4) (1999) 363–368.
[16] W.G. Characklis, M.J. Nevimons, B.F. Picologlou, Influence of fouling biofilms on heat transfer, Heat Transf. Eng. 3 (1) (2007) 23–37.
[17] I.H. Bell, E.A. Groll, Air-side particulate fouling of microchannel heat exchangers: experimental comparison of air-side pressure drop and heat transfer with plate-fin heat exchanger, Appl. Therm. Eng. 31 (5) (2011) 742–749.
[18] L. Yang, J.E. Braun, E.A. Groll, The impact of fouling on the performance of filter?evaporator combinations, Int. J. Refrig. 30 (3) (2007) 489–498.
[19] Y.C. Ahn, J.M. Cho, H.S. Shin, Y.J. Hwang, C.G. Lee, J.K. Lee, H.U. Lee, T.W. Kang, An experimental study of the air-side particulate fouling in fin-and-tube heat exchangers of air conditioners, Kor. J. Chem. Eng. 20 (5) (2003) 873–877.
[20] J.C. Luongo, S.L. Miller, Ultraviolet germicidal coil cleaning: decreased surface microbial loading and resuspension of cell clusters, Build. Environ. 105 (2016) 50–55.
[21] H. Pu, G. Ding, X. Ma, H. Hu, Y. Gao, Effects of biofouling on air-side heat transfer and pressure drop for finned tube heat exchangers, Int. J. Refrig. 32 (5) (2009) 1032–1040.
[22] W.P. Bahnfleth, UVGI in air handlers, ASHRAE J. 53 (4) (2011) 70–72.
[23] Meteorological Service Singapore, http://www.weather.gov.sg/climate-climate-of-singapore/.
[24] U.S Department of Energy, Chilled-Water-Based Air Cooling Coil, EnergyPlus Engineering Reference, 2014.
[25] O. Morisot, D. Marchio, P. Stabat, Simplified model for the operation of chilled water cooling coils under nonnominal conditions, HVAC&R Res. 8 (2) (2002) 135–158.
[26] M.J. Brandemuehl, S. Gabel, I. Andresen, HVAC2 toolkit: algorithms and subroutines for secondary HVAC system energy calculations, Atlanta, GA : American Society of Heating, Refrigerat. Air Condition. Eng. (1993).
[27] J. Firrantello, W.P. Bahnfleth, R. Montgomery, P. Kremer, Field study of energy use-related effects of ultraviolet germicidal irradiation of a cooling coil, ASHRAE Trans. 122 (1) (2016) 8.
[28] M. Wetter, Simulation Model: finned water-to-air coil without condensation, LBNL 42355 (1999).
[29] V. Gnielinski, New equation for heat and mass transfer in turbulent pipe and channel flow, Int. Chem. Eng. 16 (1976) 359–368.
[30] ASHRAE, ASHRAE guideline 2–1986 (RA96): engineering analysis of experimental data, atlanta, GA : American Society of Heating, Refrigerat. Air Condition. Eng. (2004).